

This paper is published as part of a *Dalton Transactions* themed issue on:

## Metal Anticancer Compounds

Guest Editor Peter Sadler

University of Warwick, UK

Published in [issue 48, 2009](#) of *Dalton Transactions*



Image reproduced with permission of Chi-Ming Che

Articles published in this issue include:

### PERSPECTIVES:

[Non-traditional platinum compounds for improved accumulation, oral bioavailability, and tumor targeting](#)

Katherine S. Lovejoy and Stephen J. Lippard, *Dalton Trans.*, 2009, DOI: 10.1039/b913896j

[Metal complexes as photochemical nitric oxide precursors: Potential applications in the treatment of tumors](#)

Alexis D. Ostrowski and Peter C. Ford, *Dalton Trans.*, 2009, DOI: 10.1039/b912898k

[Novel and emerging approaches for the delivery of metallo-drugs](#)

Carlos Sanchez-Cano and Michael J. Hannon, *Dalton Trans.*, 2009, DOI: 10.1039/b912708a

### HOT ARTICLE:

[Iron\(III\) complexes of fluorescent hydroxamate ligands: preparation, properties, and cellular processing](#)

Antonia J. Clarke, Natsuho Yamamoto, Paul Jensen and Trevor W. Hambley, *Dalton Trans.*, 2009, DOI: 10.1039/b914368h

Visit the *Dalton Transactions* website for more cutting-edge inorganic and bioinorganic research  
[www.rsc.org/dalton](http://www.rsc.org/dalton)

# Inert ruthenium half-sandwich complexes with anticancer activity

Eric Meggers,<sup>\*a,c</sup> G. Ekin Atilla-Gokcumen,<sup>a</sup> Katharina Gründler,<sup>b</sup> Corazon Frias<sup>b</sup> and Aram Prokop<sup>\*b</sup>

Received 28th August 2009, Accepted 15th October 2009

First published as an Advance Article on the web 2nd November 2009

DOI: 10.1039/b917792b

In this study, we investigate the anticancer properties of an inert half-sandwich metal complex scaffold. UV melting experiments with duplex DNA and <sup>1</sup>H-NMR experiments with 9-ethylguanine reveal that the apoptotic ruthenium complex **DW12** does not interact with DNA. On the other hand, diminishing the kinase inhibition properties of **DW12** by methylating the maleimide nitrogen (**DW12-Me**) abolishes the anticancer activity. Furthermore, the incorporation of a fluorine into the pyridine moiety (**NP309**) improves the IC<sub>50</sub> value for glycogen synthase kinase 3 (GSK-3) and at the same time the cytotoxicity, implying that the anticancer activity correlates with the inhibition of GSK-3 and maybe other not yet identified kinases. We demonstrate in Burkitt-like lymphoma (BJAB) cells that **NP309** is not necrotic but induces apoptosis and that this apoptosis is mediated by a loss of the mitochondrial membrane potential, caspase-9 processing, and is partly dependent on Bcl-2 expression. In addition, **NP309** efficiently induces apoptosis in vincristine- and cytarabine-resistant human B-cell precursor cell lines.

## Introduction

Altering cell fate with small synthetic compounds is one of the key strategies in cancer therapy. Typically, in the case of inorganic anticancer agents, the metal is directly involved in the mode of action either through coordination chemistry or redox processes.<sup>1</sup> On the other hand, we have recently demonstrated the astonishing kinase inhibition and anticancer properties of the chemically inert ruthenium half sandwich complex **DW12** (Fig. 1).<sup>2–4</sup> Being highly potent for GSK-3 and Pim1, and probably some unidentified kinases, **DW12** induces significant biological responses. It is a nanomolar activator of the wnt signaling pathway in mammalian cells, exhibits strong pharmacological effects during the development of frog embryos, and is highly antiproliferative and apoptotic in melanoma cells.<sup>3,5</sup> Replacing ruthenium with osmium in this organometallic kinase inhibitor scaffold afforded the isostructural complex **DW12-Os** (Fig. 1) with almost indistinguishable biological activities.<sup>6</sup> Thus, we have strong evidence that the role of the metal in **DW12** and **DW12-Os** is solely structural and the biological effects of these compounds are due to their shape rather than the reactivity of the metal center.

Here we demonstrate that **DW12** does indeed not interact with DNA and that the cytotoxic and apoptotic effect of the compound **DW12** is instead due to its ability to inhibit the activity of protein kinases. In fact, we report that the fluorinated derivative **NP309** (Fig. 1), an improved kinase inhibitor, displays even further enhanced antiproliferative activities. We demonstrate in Burkitt-like lymphoma (BJAB) cells that **NP309** is not necrotic but induces apoptosis, mediated by a loss of the mitochondrial membrane

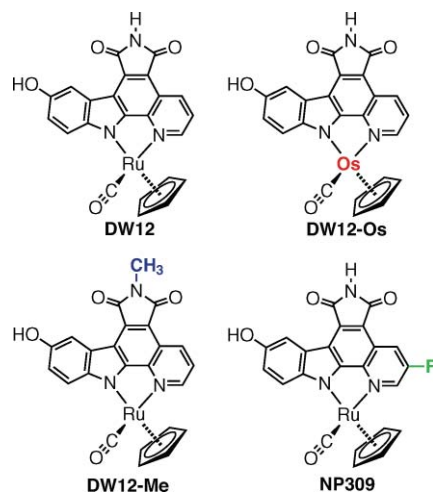


**Fig. 1** **DW12**, **DW12-Os**, **NP309**, but not **DW12-Me**, are highly cytotoxic and apoptotic in cancer cell culture. All complexes are racemic but only one enantiomer is shown.

potential, caspase-9 processing, and in part dependent on Bcl-2 expression.

## Results and discussion

### Investigation of interaction with DNA

DNA-reactive anticancer metal complexes often target the N-7 nitrogen of the guanine bases and we therefore used the reaction with 9-ethylguanine (9-EtG) as a simple model system in order to investigate the coordinative interaction of **DW12** with DNA.<sup>7</sup> Accordingly, **DW12** (2.5 mM) was incubated with 9-EtG (2.5 mM) at room temperature in 10% D<sub>2</sub>O–DMSO-d<sub>6</sub> and the interaction was followed by <sup>1</sup>H-NMR. As can be seen in Fig. 2, no reaction took place between 9-EtG and **DW12** within 48 h under these conditions. This experiment supports the notion that **DW12** is inert towards the coordination to nucleobases. As recently

<sup>a</sup>Department of Chemistry, University of Pennsylvania, 231 S. 34<sup>th</sup> Street, Philadelphia, PA 19104, USA

<sup>b</sup>Kliniken der Stadt Köln gGmbH, Neufelder Str. 34, 51067 Köln, Germany. E-mail: prokopa@kliniken-koeln.de; Fax: +49 221 89075395; Tel: +49 221 89075158

<sup>c</sup>Fachbereich Chemie, Hans-Meerwein-Strasse, 35032 Marburg, Germany. E-mail: meggers@chemie.uni-marburg.de; Fax: +49 6421 2822189; Tel: +49 6421 2821534

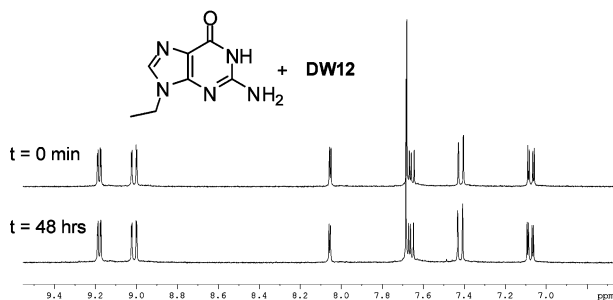


**Fig. 2**  $^1\text{H-NMR}$  spectra of a solution of **DW12** (2.5 mM) and 9-EtG (2.5 mM) at timepoint 0 and after 48 h (DMSO- $d_6$ : $\text{D}_2\text{O}$  9:1). Only the aromatic region is shown.

demonstrated, **DW12** is stable in cell culture medium and in the presence of mM concentrations of thiols,<sup>3</sup> thus further indicating that a reversible binding of **DW12** to a biomolecular target is responsible for its biological activity.

**DW12** contains a hydrophobic planar pyridocarbazole moiety which might be able to interfere with cellular function by intercalating into DNA.<sup>8</sup> In order to rule out this mode of action, we investigated the interaction of **DW12** with a synthetic 15mer DNA duplex (5'-TACAACAATAATGTG-3') by temperature-dependent UV spectroscopy at 260 nm. Accordingly, we measured the melting temperatures of the DNA duplex (2  $\mu\text{M}$ ) in the presence of different concentrations of **DW12** and found that the melting temperature of 40.0  $^\circ\text{C}$  was not affected by **DW12** within experimental error ( $\pm 0.5$   $^\circ\text{C}$ ) in the concentration range of 0 to 16  $\mu\text{M}$ , thus clearly indicating that **DW12** does not have any significant affinity for duplex DNA at biologically relevant concentrations. This might be due to a lack of positive charge in the metal complex which would be necessary for an electrostatic attraction to the polyanionic DNA. Thus, it can be concluded that **DW12** neither coordinates to DNA nucleobases nor intercalates into duplex DNA.

### Effect of imide methylation on cytotoxicity and apoptosis

We have previously established that **DW12** is highly cytotoxic to certain melanoma cell lines and that this effect is at least in part due to p53-induced apoptosis, initiated by the inhibition of the protein kinase GSK-3 $\beta$ .<sup>5</sup> In order to differentiate between cytotoxicity due to kinase inhibition or an unrelated reactivity of the organometallic moiety, we investigated the cytotoxic and apoptotic effect of the methylated derivative **DW12-Me**. This imide methylation leaves the coordination sphere of the ruthenium complex unaffected but at the same time abolishes the inhibition of most protein kinases by blocking a key hydrogen bond within the ATP-binding site. Indeed, **DW12-Me** is less potent for GSK-3 by almost four orders of magnitude compared to the parent compound **DW12**.<sup>3</sup> Thus, if the ruthenium center is in fact not responsible for the biological effect of **DW12** but solely serves as a structural scaffold for establishing strong binding to some protein kinases, **DW12-Me** should display a significantly diminished cytotoxicity.

In order to address this issue, we first tested the effect of methylation (**DW12** $\rightarrow$ **DW12-Me**) on the cytotoxicity in colon carcinoma HCT-116 cells. The compounds **DW12** and **DW12-Me** were incubated with HCT-116 for 72 h at different concentrations

varying from 0.03  $\mu\text{M}$  to 10  $\mu\text{M}$  and cell survival in each cell population was determined with the MTT method. As shown in Fig. 3, **DW12** exhibited a significantly higher cytotoxicity than **DW12-Me** with an  $\text{LC}_{50}$  value of around 0.6  $\mu\text{M}$  for **DW12**, whereas more than 80% of cells were alive at the highest tested concentration of 10  $\mu\text{M}$  **DW12-Me** (Fig. 3).

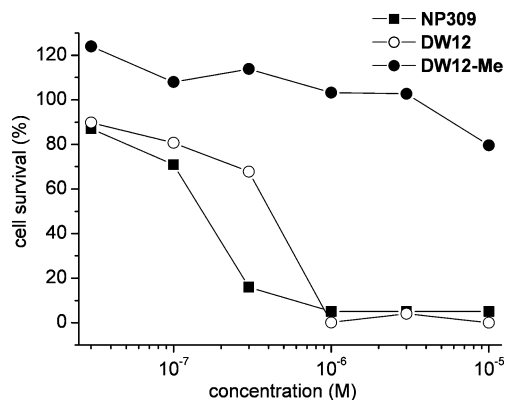


**Fig. 3** Cytotoxicity of **DW12**, **DW12-Me**, and **NP309** in HCT-116 cells. Cells were incubated with different concentrations of ruthenium compounds for 72 h and cell survival was measured with the MTT method.

Next, we compared the apoptotic properties of **DW12** and **DW12-Me**. A typical consequence of apoptosis is the formation of hypodiploid DNA fragments, the end product of the apoptotic cascade. We therefore quantified the induction of apoptosis by incubating HCT-116 cells with 1  $\mu\text{M}$  **DW12** or **DW12-Me** for 24 h, followed by analyzing the DNA content with flow cytometry after propidium iodide staining. Fig. 4 depicts the results of the cell cycle analysis in which significant differences were observed in cellular responses to **DW12** and **DW12-Me** treatment. Whereas **DW12** induced strong apoptosis with 49% of the cells in the sub- $\text{G}_1$  phase, **DW12-Me** did not differ significantly from control cells which were treated with 1% DMSO only (13% and 14% sub- $\text{G}_1$  phase, respectively), demonstrating that **DW12** induces strongly apoptosis in HCT-116, but not **DW12-Me**.

These experiments suggest that it is the ability of **DW12** to inhibit protein kinases which is responsible for its cytotoxic and apoptotic effects.

### NP309, a protein kinase inhibitor with improved anticancer properties

Several recent studies reveal a formerly unrecognized role of GSK-3 in tumor cell survival and proliferation.<sup>5,9-14</sup> For example, it was found that colon cancer cells display high levels of GSK-3 $\beta$  and its active form phospho-GSK-3 $\beta^{\text{Tyr}216}$ .<sup>12</sup> Furthermore, it was demonstrated in colon cancer cells such as HCT-116 that an inhibition of GSK-3 $\beta$  activity by pharmacological inhibitors or elimination of GSK-3 $\beta$  by RNA interference (RNAi) induced apoptosis and attenuated proliferation of colon cancer cells.<sup>12</sup> Recent studies by some of us<sup>5</sup> and others<sup>11</sup> suggest that GSK-3 $\beta$  cooperates with Mdm2 to directly regulate the export of the tumor suppressor protein p53 from the nucleus *via* phosphorylation of p53, thus explaining at least in part the apoptotic properties of GSK-3 inhibitors such as the organometallic compound **DW12**.

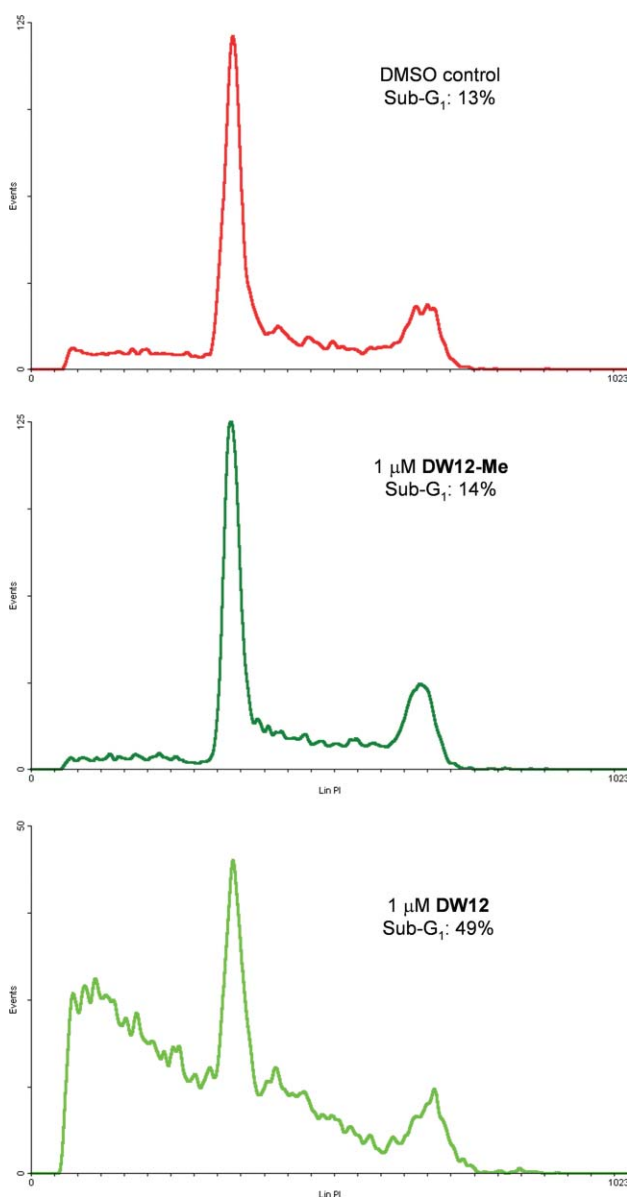


**Fig. 4** Cell cycle analysis reveals that **DW12** but not **DW12-Me** strongly induces apoptosis. HCT-116 cells were treated with 1  $\mu\text{M}$  **DW12** or **DW12-Me**. Cells were then harvested and ethanol-fixed before stained with propidium iodide and analyzed using flow cytometry. DMSO was used as a control sample.

Since the anticancer activity of the organometallic scaffold **DW12** displays an apparent correlation with its ability to inhibit GSK-3, we sought to enhance the anticancer activity further by improving the kinase inhibition properties. As reported recently, the introduction of an additional fluorine at the pyridine moiety (**DW12**→**NP309**) improves the binding affinity by almost one order of magnitude, affording a picomolar inhibitor for GSK-3 $\beta$  (**DW12**:  $\text{IC}_{50}$  = 2 nM; **NP309**,  $\text{IC}_{50}$  = 0.3 nM at 100  $\mu\text{M}$  ATP).<sup>15</sup> Indeed, following the observed trend, **NP309** shows a higher cytotoxicity in HCT-116 with an  $\text{LC}_{50}$  value of around 200 nM, compared to 600 nM for **DW12** (Fig. 3), once more demonstrating the correlation between the anticancer activity and protein kinase inhibition of the here discussed organometallic scaffold.

### No induction of necrosis by NP309

Depending on their concentration, many cytostatic substances cause undesired necrotic cell death accompanied by membrane damage. In order to exclude unspecific cell death *via* necrosis, lactate dehydrogenase (LDH) release was determined. Early LDH release is characteristic for necrotic cell death, while apoptotic cells maintain their membrane integrity and do not emit large intracellular proteins like LDH. We therefore investigated LDH release in Burkitt-like lymphoma (BJAB) cells by incubating BJAB cells with different concentrations of the complex **NP309** and measuring the LDH release into the culture medium after 1 h. As illustrated in Fig. 5, LDH release was very low and the cell viability was not significantly reduced after 1 h of incubation with **NP309** at cytotoxic concentrations. The results indicate that necrosis does not have a significant impact on the potency of **NP309**.

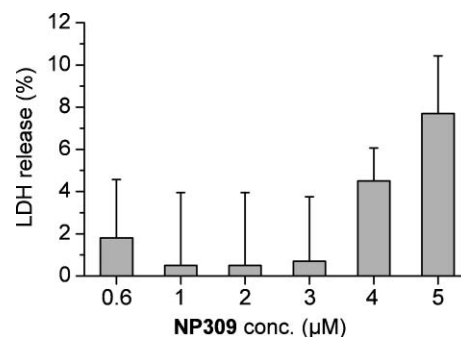


**Fig. 5** Lactate dehydrogenase (LDH) release assay to evaluate necrotic properties of **NP309**. BJAB cells were incubated with the indicated concentration of **NP309** for 1 h and the LDH release measured. LDH activity of lysed cells was used as a 100% control. Values are given in %  $\pm$  SD ( $n$  = 3).

### Induction of apoptosis by NP309

Similar to its effect on HCT-116, **NP309** showed efficient antiproliferate properties in BJAB cells (Fig. 6). To further investigate the **NP309**-induced induction of apoptosis, a flow cytometric cell cycle analysis was performed after incubating BJAB cells with **NP309** for 72 h. The results are shown in Fig. 7a and confirm a dose-dependent induction of apoptosis in BJAB cells after the treatment with **NP309**. **NP309** potently induced DNA fragmentation in up to 80% of the cells and apoptosis induction was concentration-dependent with a half-maximum concentration of about 4  $\mu\text{M}$ . These data verify specific induction of apoptosis by **NP309**.

To determine the involvement of the mitochondrial pathway in the induction of apoptosis, mitochondrial activation after treatment of BJAB cells with **NP309** for 48 h was measured. Exposure to **NP309** resulted in a dose-dependent loss of the mitochondrial membrane potential determined by staining with the dye JC-1 (Fig. 7b).<sup>16</sup> Additionally, the caspase-9 activation was investigated for a more specific proof of the intrinsic pathway. As illustrated in Fig. 7c, the procaspase-9 degradation was analyzed by Western blot analysis after incubating the BJAB cells with 3  $\mu\text{M}$  and 3.5  $\mu\text{M}$  **NP309**, revealing a reduction in procaspase-9 levels by **NP309**. Furthermore, Fig. 7d demonstrates that induction of apoptosis by **NP309** is partly dependent on Bcl-2 levels, but

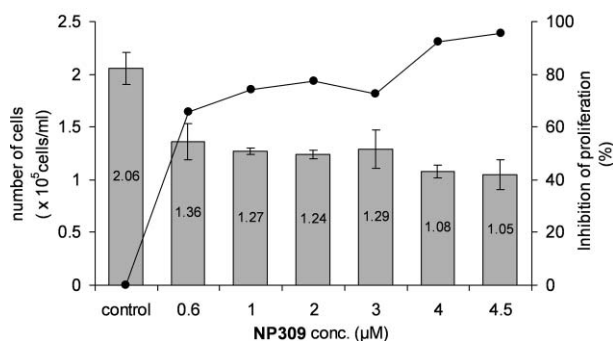


**Fig. 6** Antiproliferative effect of NP309 in BJAB cells. Inhibition of cell proliferation after treatment with NP309 for 24 h as measured by a CASY cell counter. Untreated cells served as the control. Bars indicate the number of cells after 24 h incubation in units of  $10^5$  cells  $\text{ml}^{-1} \pm \text{SD}$  ( $n = 3$ ). The line chart indicates the inhibition of cell proliferation in % of the control.

overcomes the Bcl-2-mediated block of apoptosis. The protein Bcl-2 is a strong antiapoptotic protein of the mitochondrial pathway and tumor cells, which overexpress Bcl-2, are often resistant to cytostatic drugs.<sup>17</sup> Here we used the melanoma cell line MelHO transfected with the pIRES plasmid (MelHO-pIRES) and with the Bcl-2 cDNA in pIRES, respectively (MelHO bcl-2). MelHO Bcl-2 cells produce a 30-fold overexpression of Bcl-2 compared to MelHO pIRES cells (data not shown) and are less prone to the induction of apoptosis by NP309 (Fig. 7d). Indeed, as the data in Fig. 7d reveal, Bcl-2 overexpression reduced the

levels of apoptosis induced by NP309, but did not completely block it. Thus, our investigations clearly demonstrate that NP309 induces apoptosis in a Bcl-2 dependent manner and triggers the mitochondrial pathway of apoptosis.

### Induction of apoptosis by NP309 in drug resistant cell lines

The identification of new generations of anticancer compounds that overcome the resistance of cancer cells against currently used drugs is an important goal in clinical oncology. Therefore, the effect of NP309 on vincristine (Vcr)- and daunorubicin (Dau)-resistant cancer cell lines was tested. Regular leukemia cells (Nalm6) and Vcr-resistant Nalm6 cells, as well as Dau-resistant Nalm6 cells were treated with NP309 for 72 h and apoptosis induction was determined by flow cytometric measurements. In Fig. 8a the strong apoptosis induction in Vcr-resistant leukemia cells is depicted, whereas the apoptosis induction in Dau-resistant leukemia cell is displayed in Fig. 8b. Thus, it can be concluded that these *in vitro* experiments with the human B-cell precursor leukemia cell line Nalm6 indicate that NP309 overcomes drug resistance in vincristine-resistant and daunorubicin-resistant cells.

### Conclusions

In conclusion, we here demonstrated that ruthenium complex DW12 does not interact with nucleic acids and that its anticancer effects are instead due to its inhibition of protein kinases. DW12 and the even more cytotoxic derivative NP309 are thus members of

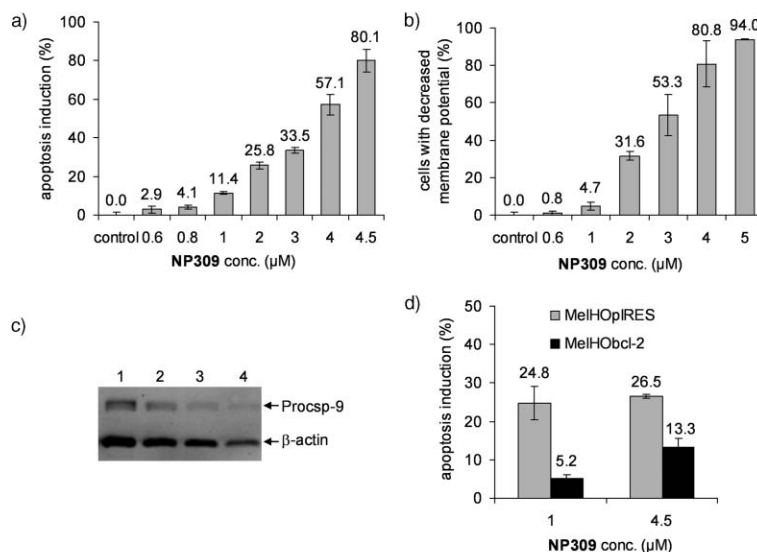


**Fig. 7** Probing the induction of apoptosis by NP309 via the intrinsic pathway. a) Induction of apoptosis measured by DNA fragmentation after treatment of BJAB cells with NP309 for 72 h. Nuclear DNA fragmentation was quantified by flow cytometric determination of hypodiploid DNA. Data are given in percentage hypoploidy (sub- $G_1$ )  $\pm \text{SD}$  ( $n = 3$ ), which reflects the number of apoptotic cells. b) Influence of NP309 on the membrane potential: The mitochondrial permeability transition was measured by flow cytometric analysis in BJAB cells after treatment with various concentrations of NP309 for 48 h. Values of the mitochondrial permeability transition are given as the fraction of cells with decreased membrane potential in %  $\pm \text{SD}$  ( $n = 3$ ). c) Procaspase-9 degradation: BJAB cells were incubated for 48 h with 2.2  $\mu\text{M}$  epirubicin (lane 2, positive control), 3  $\mu\text{M}$  NP309 (lane 3), and 3.5  $\mu\text{M}$  NP309 (lane 4). Lane 1 displays untreated cells. Cytosolic proteins (20  $\mu\text{g}$ ) were separated by SDS-PAGE, subjected to Western blot analysis, and immunoblotted with an anticaspase-9 antibody. The position of the 47 kDa procaspase-9 (Procsp-9) is indicated. Equal loading and blotting was verified by detection of the 43 kDa  $\beta$ -actin. d) Apoptosis induction in the multidrug-resistant melanoma cell line MelHO bcl-2 (stable transfection and 30-fold overexpression of Bcl-2). DNA fragmentation was measured after 72 h by flow cytometric analysis. Data are given in percentage hypoploidy (sub- $G_1$ )  $\pm \text{SD}$  ( $n = 3$ ), which reflects the number of apoptotic cells. As a control, the vector-transfected MelHO clone (MelHO pIRES) was used.

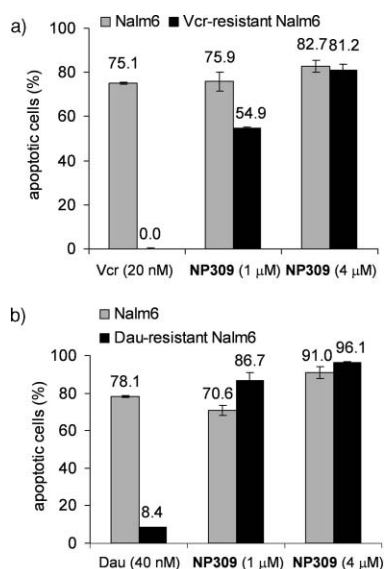


**Fig. 8** NP309-induced apoptosis in vincristine (Vcr)-resistant and daunorubicin (Dau)-resistant leukemia cells. Apoptosis was determined by DNA fragmentation in regular leukemia cells (Nalm6) and a) Vcr-resistant Nalm6 cells, as well as b) Dau-resistant Nalm6 cells after an incubation period of 72 h with various concentrations of the indicated drugs. Data are given in percentage hypodiploidy (sub-G<sub>1</sub>) ± SD (*n* = 3), which reflects the number of apoptotic cells.

a new class of anticancer metal complexes in which the metal is not directly involved in the mode of action. NP309 efficiently triggers the mitochondrial pathway of apoptosis and shows promising anticancer activities in some drug resistant cell lines.

## Experimental

### Synthesis

The synthesis of DW12,<sup>3</sup> DW12-Me<sup>3</sup> and NP309<sup>15</sup> has been reported recently.

### Reaction of DW12 with 9-EtG

A solution of DW12 (2.5 mM) and 9-EtG (2.5 mM) was incubated at room temperature in DMSO-d<sub>6</sub> with 10% D<sub>2</sub>O. <sup>1</sup>H-NMR spectra (Bruker DMX-360, 360 MHz) were taken after different time intervals.

### Interaction of DW12 with duplex DNA

Solutions containing 2 μM of a 15mer DNA duplex (5'-TACAACAATAATGTG-3' plus complementary strand) and various concentrations of DW12 (0–16 μM) 10 mM phosphate buffer pH 7.0, 50 mM NaCl and 20% DMSO were prepared. UV-monitored melting experiments were carried out in 1 cm path length quartz cells (sample volume 200 μl) on a Beckman DU800 spectrophotometer with a thermo programmer. Melting curves were monitored at 260 nm with a heating rate of 1 °C min<sup>-1</sup> and the melting temperature (*T<sub>m</sub>* values) were calculated by using a non-linear fit of the melting curves.

### Cytotoxicity measurements in HCT-116

Human colon cancer cells HCT-116 were maintained in DMEM supplemented with 10% FBS at 37 °C under an atmosphere of 5% CO<sub>2</sub> and constant humidity. Cells were plated into 96-well plates (2500–3000 cells/well) and left to attach for 24 h. Afterwards, different concentrations of DW12, DW12-Me, or NP309 were added and cells incubated with the compounds for 72 h. As a control, the same number of cells was treated with 1% DMSO. After the incubation period, the medium was replaced with 200 μL of fresh medium and 20 μL 5 mg ml<sup>-1</sup> of 3-(4,5-dimethylthiazol-2-yl)-2,5-diphenyltetrazolium bromide (MTT). Cells were incubated with MTT for 3 h and after that time 175 μL of medium was removed and 90 μL of DMSO was added to solubilize the resulting purple crystals. Absorbance of each well was measured at 550 nm. Cell survival at different inhibitor concentrations was calculated as a percentage of the control absorbance. Each experiment was repeated in quadruple.

### Cell cycle analysis in HCT-116

Approximately 1 × 10<sup>6</sup> HCT-116 cells were grown adherently for 24 h. After incubating with 1 μM DW12 or DW12-Me for 24 h, the cells were harvested. They were washed and resuspended (250 μL) in cold PBS. Cells were fixed by adding 2 mL of 70% EtOH and incubated overnight at 4 °C. Next morning, the cells were spun down and resuspended in 200 μl propidium iodide solution, containing 40 μg ml<sup>-1</sup> propidium iodide, 100 μg ml<sup>-1</sup> RNase in PBS and incubated at 37 °C for 30 min in the dark to label intracellular DNA. The cell cycle profile was obtained by analyzing 15 000 cells. Apoptosis was defined by the percentage of cells in the sub-G<sub>1</sub> fraction of the cell cycle.

### Cell culture with BJAB and Nalm6 cells

BJAB (Burkitt-like lymphoma) and Nalm6 (human B cell precursor leukemia) cells were cultured at 37 °C in RPMI 1640 (GIBCO, Invitrogen) supplemented with 10% heat-inactivated FCS, 10<sup>5</sup> U/L penicillin, 0.1 g L<sup>-1</sup> streptomycin, and 0.56 g L<sup>-1</sup> L-glutamine. The cells were subcultured every 3–4 days by diluting the cells to a concentration of 1 × 10<sup>5</sup> cells ml<sup>-1</sup>. DMEM was used instead of RPMI 1640 for MelHO only. Twenty four hours before the assay setup, cells were cultured to a concentration of 3 × 10<sup>5</sup> cells ml<sup>-1</sup> to ascertain standardized growth conditions. For the experiments cells were diluted to a concentration of 1 × 10<sup>5</sup> cells ml<sup>-1</sup> immediately before addition of the complexes.

### LDH release assay<sup>18</sup>

BJAB cells were incubated with various concentrations of NP309 for 1 h at 37 °C and LDH activity measured in the cell culture supernatants using the Cytotoxicity Detection Kit from Boehringer Mannheim. The supernatants were centrifuged at 1500 rpm for 5 min. Then, 20 μl of cell-free supernatants were diluted with 80 μl phosphate-buffered saline (PBS) and 100 μl reaction mixture. Time-dependent formation of the reaction product was quantified photometrically at 490 nm. The maximum amount of LDH activity released by the cells was determined by lysis of the cells using 0.1% Triton X-100 in culture medium and set as 100%.

## Determination of cell viability in BJAB and Nalm6 cells

Cell viability was determined by CASY® (Cell counter and Analyzer System of Innovatis, Bielefeld, Germany). Settings were specifically defined for the requirements of the cells used. The cell concentration was analyzed simultaneously in three different size ranges: cell debris, dead cells, and viable cells. After a 24 h incubation period at 37 °C, cells were resuspended properly, and 100 µl of each well was diluted in 10 ml CASYton (ready-to-use isotonic saline solution) for an immediate automated counting of the cells.

## Measurement of DNA fragmentation in BJAB cells

Apoptotic cell death was determined by a modified cell-cycle analysis which detects DNA fragmentation at the single-cell level as described previously.<sup>19,20</sup> After a 72 h incubation period at 37 °C, cells were collected by centrifugation at 1500 rpm for 5 min, washed with PBS at 4 °C and fixed in PBS–formaldehyde (2% v/v) on ice for 30 min. After fixation, cells were incubated with EtOH–PBS (2:1 v/v) for 15 min, pelleted and resuspended in PBS containing 40 µg ml<sup>-1</sup> RNase A. RNA was digested for 30 min at 37 °C, after which the cells were pelleted once again and finally resuspended in PBS containing 50 µg ml<sup>-1</sup> propidium iodide. Nuclear DNA fragmentation was quantified by flow cytometric determination of hypodiploid DNA (fluorescence-activated cell sorting, FACS). Data were collected and analyzed using a FACScan (Becton Dickinson, Heidelberg, Germany) apparatus equipped with CELL Quest software. Data are given in % hypodiploidy (sub-G<sub>1</sub>), which reflects the number of apoptotic cells.

## Measurement of the mitochondrial permeability transition in BJAB cells

After an incubation period of 48 h with various concentrations of the complexes, cells were collected by centrifugation at 1500 rpm at 4 °C for 5 min. The mitochondrial permeability transition was then determined by staining the cells with 5,5',6,6'-tetrachlor-1,1',3,3'-tetraethyl benzimidazolylcarbocyanine iodide (JC-1, Molecular Probes). Cells were resuspended in 500 µl phenol-red-free RPMI 1640 without supplements, and JC-1 was added to give a final concentration of 2.5 µg ml<sup>-1</sup>. The cells were incubated for 30 min at 37 °C with moderate shaking. Control cells were likewise incubated in the absence of JC-1 dye. The cells were harvested by centrifugation at 1500 rpm and 4 °C for 5 min, washed with ice-cold PBS, and resuspended in 200 µl PBS at 4 °C. Mitochondrial permeability transition was then quantified by flow cytometric determination of the cells with decreased fluorescence, that is, with mitochondria displaying a lower membrane potential. Data were collected and analyzed using a FACScan (Becton Dickinson, Heidelberg, Germany) apparatus equipped with CELL Quest software. Data are given in percentage of the cells with low mitochondrial membrane potential, which reflects the number of cells undergoing mitochondrial apoptosis.

## Immunoblotting

After incubation for 48 h with different concentrations of NP309, BJAB cells were washed twice with PBS and lysed in buffer

containing 10 mM Tris–HCl, pH 7.5, 300 mM NaCl, 1% Triton X-100, 2 mM MgCl<sub>2</sub>, 5 µM EDTA, 1 µM pepstatin, 1 µM leupeptin and 0.1 mM phenylmethylsulfonyl fluoride (PMSF). Protein concentration was determined using the bicinchoninic acid assay<sup>21</sup> from Pierce (Rockford, IL, USA), and equal amounts of protein were separated by SDS-PAGE.<sup>22</sup> Immunoblotting was performed at 1 mA cm<sup>-2</sup> for 1 h in a Transblot SD cell (BioRad, München, Germany). The membrane was blocked for 1 h in PBST (PBS, 0.05% Tween-20) containing 5% non-fat dry milk and incubated with primary anti-mouse caspase-3 (Santa Cruz, CA, USA) antibody over night or with anti-mouse caspase-9 (RD Systems) for 1 h. After the membrane was washed in PBST, secondary antibody (anti-mouse HRP conjugated, RD Systems) in PBST was applied for 1 h. After washing, the protein bands were detected using the ECL enhanced chemiluminescence system (Amersham, Braunschweig, Germany).

## Acknowledgements

We thank the US National Institutes of Health for support (CA114046). We thank the Dr Kleist-Stiftung Berlin for financial support. We thank Jeffrey S. Faust from the flow cytometry facilities at the Wistar Institute (Philadelphia, USA) for support with some cell cycle analyses and Jürgen Eberle (Charité Berlin) for the Bcl-2-transfected MelHO-cells.

## References

- 1 Metal-based therapeutics: (a) Z. Guo and P. J. Sadler, *Angew. Chem., Int. Ed.*, 1999, **38**, 1512–1531; (b) M. J. Clarke, *Coord. Chem. Rev.*, 2002, **232**, 69–93; (c) K. H. Thompson and C. Orvig, *Science*, 2003, **300**, 936–939; (d) P. J. Dyson and G. Sava, *Dalton Trans.*, 2006, 1929–1933; (e) W. H. Ang and P. J. Dyson, *Eur. J. Inorg. Chem.*, 2006, 4003–4018; (f) D. Chatterjee, A. Mitra and G. S. De, *Platinum Met. Rev.*, 2006, **50**, 2–12; (g) T. W. Hambley, *Science*, 2007, **318**, 1392–1393; (h) T. W. Hambley, *Dalton Trans.*, 2007, 4929–4937.
- 2 E. Meggers, G. E. Atilla-Gokcumen, H. Bregman, J. Maksimoska, S. P. Mulcahy, N. Pagano and D. S. Williams, *Synlett*, 2007, 1177–1189.
- 3 D. S. Williams, G. E. Atilla, H. Bregman, A. Arzoumanian, P. S. Klein and E. Meggers, *Angew. Chem., Int. Ed.*, 2005, **44**, 1984–1987.
- 4 J. É. Debreczeni, A. N. Bullock, G. E. Atilla, D. S. Williams, H. Bregman, S. Knapp and E. Meggers, *Angew. Chem., Int. Ed.*, 2006, **45**, 1580–1585.
- 5 K. S. M. Smalley, R. Contractor, N. K. Haass, A. N. Kulp, G. E. Atilla-Gokcumen, D. S. Williams, H. Bregman, K. T. Flaherty, M. S. Soengas, E. Meggers and M. Herlyn, *Cancer Res.*, 2007, **67**, 209–217.
- 6 J. Maksimoska, D. S. Williams, G. E. Atilla-Gokcumen, K. S. M. Smalley, P. J. Carroll, R. D. Webster, P. Filippakopoulos, S. Knapp, M. Herlyn and E. Meggers, *Chem.–Eur. J.*, 2008, **14**, 4816–4822.
- 7 For related experiments with 9-EtG, see for example: A. F. A. Peacock, A. Habtemariam, S. A. Moggach, A. Prescimone, S. Parsons and P. J. Sadler, *Inorg. Chem.*, 2007, **46**, 4049–4059.
- 8 For indolocarbazoles which interact with DNA, see: M. Prudhomme, *Eur. J. Med. Chem.*, 2003, **38**, 123–140.
- 9 P. Watcharasi, G. N. Bijur, J. W. Zmijewski, L. Song, A. Zmijewska, X. Chen, G. V. Johnson and R. S. Jope, *Proc. Natl. Acad. Sci. U. S. A.*, 2002, **99**, 7951–7955.
- 10 P. Watcharasi, G. N. Bijur, L. Song, J. Zhu, X. Chen and R. S. Jope, *J. Biol. Chem.*, 2003, **278**, 48872–48879.
- 11 R. Kulikov, K. A. Boehme and C. Blattner, *Mol. Cell. Biol.*, 2005, **25**, 7170–7180.
- 12 A. Shakoori, A. Ougolkov, Z. W. Yu, B. Zhang, M. H. Modarressi, D. D. Billadeau, M. Mai, Y. Takahashi and T. Minamoto, *Biochem. Biophys. Res. Commun.*, 2005, **334**, 1365–1373.
- 13 J. Tan, L. Zhuang, H.-S. Leong, N. Gopalakrishna, I. Edison, T. Liu and Q. Yu, *Cancer Res.*, 2005, **65**, 9012–9020.

- 
- 14 Z. Wang, K. S. Smith, M. Murphy, O. Piloto, T. C. P. Somerville and M. L. Cleary, *Nature*, 2008, **455**, 1205–1210.
- 15 N. Pagano, J. Maksimoska, H. Bregman, D. S. Williams, R. D. Webster, F. Xue and E. Meggers, *Org. Biomol. Chem.*, 2007, **5**, 1218–1227.
- 16 M. Reers, T. W. Smith and L. B. Chen, *Biochemistry*, 1991, **30**, 4480–4486.
- 17 R. J. Youle and A. Strasser, *Nat. Rev. Mol. Cell Biol.*, 2008, **9**, 47–59.
- 18 T. Decker and L.-M. Lohmann-Matthes, *J. Immunol. Methods*, 1988, **115**, 61–69.
- 19 I. Nicoletti, G. Migliorati, M. G. Pagliacci, F. Grignani and C. A. Riccardi, *J. Immunol. Methods*, 1991, **139**, 271–279.
- 20 C. Riccardi and I. Nicoletti, *Nat. Protoc.*, 2006, **1**, 1458–1461.
- 21 P. K. Smith, R. I. Krohn and G. T. Hermanson, *Anal. Biochem.*, 1985, **150**, 76–85.
- 22 U. K. Laemmli, *Nature*, 1970, **227**, 680–685.